Water splitting reaction over $Ce_{0.15}Zr_{0.85}O_2$ driven by surface heterogeneity

Alfonsina Pappacena[1], Marta Boaro*[1], Lidia Armelao[2], Jordi Llorca[3], Alessandro Trovarelli[1]

[1] Dipartimento di Chimica, Fisica e Ambiente,
Università degli Studi di Udine, via del Cotonificio 108, 33100 Udine, Italy

[2] IENI-CNR and INSTM, Dipartimento di Scienze Chimiche,
Università di Padova, Via Marzolo 1, 35131 Padova, Italy

[3] Institut de Tècniques Energètiques and Centre for Research in Nanoengineering,
Universitat Politècnica de Catalunya, Diagonal 647, 08028 Barcelona, Spain

Abstract

The compositional and structural heterogeneity of a sample of $Ce_{0.15}Zr_{0.85}O_2$ subjected to a two-step thermochemical water splitting reaction was investigated by means of X-ray powder diffraction (XRD), X-Ray Photoelectron Spectroscopy (XPS) and High-Resolution Transmission Electron Microscopy (HRTEM) analysis. High temperature treatment under N_2 resulted in segregation of a Zr-rich monoclinic phase on one side and a Ce-rich cubic phase on the other. The treatment also led to a higher reducibility of the material compared to similar studies on Ce-rich compositions. HRTEM revealed the presence of a zirconia based superstructure that it is identifiable with an oxynitride phase Zr_2ON_2, while ceria surface enrichment was detected via XPS. H_2 yield, investigated at 800°C by pulsing water over several redox cycles, showed a six-fold increase after the first cycle remaining constant after at least three subsequent cycles. The presence of zirconia oxynitride was found to be beneficial for both the oxidation and reduction steps.

Solar thermochemical water splitting cycles (WSC) are an attractive carbon-free approach to H_2 production from water and sunlight.[1] Two-step metal oxide based cycles generate H_2 through high temperature (~1500-2000°C) reduction in inert atmosphere and the subsequent water oxidation at a lower (~400-1300°C) temperature making water splitting (WS) possible at temperatures lower than the thermodynamic value (2300°C).[2] Among many metal oxides investigated in literature, ceria is one of the most viable candidates,[3] and it can deliver pure oxygen and hydrogen according to the following two-step redox cycle [4]

$$CeO_2\,(s) \rightarrow CeO_{2-\delta}\,(s) + \delta/2\,O_2 \qquad \text{(endothermic step, T>1800°C)} \qquad (1)$$

$$CeO_{2-\delta}\,(s) + \delta H_2O\,(g) \rightarrow CeO_2\,(s) + \delta H_2\,(g) \qquad \text{(exothermic step, 400-500°C)} \qquad (2)$$

The main drawback of this cycle is that a significant reduction of ceria occurs only at temperatures higher than 1800°C, where sublimation can occur with a decrease of the yield over cycles.[5] It follows that studies on ceria-based systems have been focused on lowering the reduction temperature of the Ce^{4+}/Ce^{3+} redox couple, while maintaining the high reactivity of reduced Ce^{3+} species towards water.[3,6] The addition of high valence dopant cations, such as Zr^{4+}, proved effective in increasing the thermodynamic driving force of CeO_2 reduction at lower temperatures,[7-9] and the effect of zirconium content in the two step water splitting reaction has been widely studied.[10-14] Its presence favours CeO_2 reduction under inert atmosphere at temperatures lower than 1500°C preventing sublimation and the consequent yield loss; moreover, the increased oxygen storage of ceria-zirconia positively affects O_2 yield. On the other hand, the H_2 productivity depends on the number of exposed surface redox sites, and thus on the textural, morphological and structural properties of these materials. It was reported that in these materials the kinetics of water splitting is often hampered by gas-solid diffusion limitations due to the simultaneous occurence of sintering processes. Several efforts have been made to overcome this issue, and the change of the morphological and structural properties of the mixed oxides by introducing other dopants[15] or by using different synthesis approaches[11,16,17] was found to be beneficial.

Ceria-rich compositions have generally a good structural stability at the operating temperatures of the reduction step, while zirconia-rich compositions (Zr ≥50 mol%) are thermodynamically unstable in such conditions and undergo structural changes and phase segregation.[18] For this reason the majority of studies on the water splitting reaction over ceria-

zirconia solid solutions focused on compositions with a zirconia content in the range up to 70 mol% CeO_2,[10-17] although it has been recently reported that the occurrence of compositional heterogeneities may have a benefical effect on the H_2 production step.[11] With the aim of gaining insights into this latter aspect and of exploring the potential application of ZrO_2-rich compositions in the WS reaction, despite their thermodynamic instability, we investigate here the reactivity and structural transformations of $Ce_{0.85}Zr_{0.15}O_2$ in the reduction and oxidation step of the cycle. It is shown that the solid solution undergoes structural evolution and compositional changes during high temperature treatments, with phase segregation and the formation of a N-containing ZrO_2 rich phase. This specific structural and compositional heterogeneity is shown to be responsible for the promotion of the WS reaction in this system, and the result is an additional step torward the understanding of the structure/activity relationship in CeO_2-ZrO_2 based oxides.

$Ce_{0.15}Zr_{0.85}O_2$ solid solution was prepared through a surfactant assisted approach.[19] Figure 1a shows that the material crystallizes in a tetragonal phase (PDF # 88-2398), in agreement with its nominal stoichiometry. Textural and oxygen storage properties of the fresh sample are reported in the supplementary section. Redox behaviour, as shown by temperature programed reduction (Fig. S1) is characterized by a single broad peak of hydrogen consumption in the range of temperature 300-500 °C, with a total H_2 uptake of 2,94 mmol/gCeO_2, corresponding to a Ce^{4+}/Ce^{3+} reduction degree of ca. 84%. This is in line with results reported for samples of similar composition.[20] The fresh material was treated at 1300°C for 4 hours under N_2 flow before of the catalytic tests, in order to simulate the aging process occurring over several endothermic steps. After ageing, the surface area of the sample dropped to a negligible value due to sintering, and significant structural transformations were detected following the XRD analysis. In addition to the tetragonal phase of composition $Ce_{0.15}Zr_{0.85}O_2$, the XRD profile of aged sample (Figure 1b) identified the presence of a cubic ceria-rich and a monoclinic zirconia-rich phase, originated from segregation of the starting composition. The transformations are in agreement with those predictable from the ceria-zirconia phase stability diagram that shows the co-existence of monoclinic, tetragonal and cubic phases at 1300°C.[18] Rietveld analysis of the difractogram permitted a more precise identification of these phases and the results related to their quantification are reported in Table 1.

The surface chemical composition of the catalyst was determined by XPS analysis (see Table 1 and SI for details). The measured Zr/Ce atomic ratio is equal to *ca*. 1.8, a value significantly lower than expected for the $Ce_{0.15}Zr_{0.85}O_2$ composition (i.e. 5.6), indicating that restructuring of the material with formation of different phases also leads to a substatial ceria enrichment of

the surface. This can be explained by a preferential migration of the segregated $Ce_{0.70}Zr_{0.30}O_2$ cubic phase to the surface or subsurface region of the material.

The activity of the aged sample in two-step water splitting cycle was investigated keeping separated the endothermic and exothermic step. The endothermal reduction in N_2 flow was calculated from the weight loss recorded during 80min isothermal test at 1300°C in a thermogravimetric analyser. The total O_2 release was of 165 μmol/g, equivalent to 825 μmol/g-CeO_2. The value is comparable to that found for solid solutions richer in ceria[16], and corresponds to a $Ce(III)/Ce(IV)_{tot}$ reduction yield of 56% relative to the initial composition, which is the highest reduction degree ever obtained by ceria-zirconia oxides in this type of reaction. The high zirconia content of sample coupled with a greater number of reducible sites exposed on its surface as the result of the ceria-rich phase segregation, can explain the present finding.

The exothermal oxidation of the catalyst with water vapor pulses was carried out at 800°C in a gas analyser by following an approach similar to that reported by Petkovich et al.[11] (see supporting information for more details. Figure 2 shows the results related to six H_2/H_2O redox cycles. H_2 production, as expected, was initially low (cycle 1), due to the thermodynamic and kinetic limitations[3,17] that hinder the reoxidation process in compositions containing a great quantity of zirconia with water.

An intriguing result, which triggered further investigations, was observed at the second redox cycle when a sharp increase in the reactivity was registered and remained nearly constant over the three subsequent cycles. At these stages the H_2 yield (~100 μmoles/g) compares well with that found for most of the currently investigated ceria-zirconia compositions.[16]

In order to understand the role of the structural heterogeneity in the promotion effect of the redox behavior of the material, the sample was characterized at the atomic scale via HRTEM and XPS analysis, after aging and following the first two cycles. Figure 3A shows the HRTEM micrograph of the aged sample before the H_2/H_2O redox cycles. The inset shows that the sample was constituted by crystals from 5 up to 50 nm. Moreover, the analysis confirmed the presence of segregated phases at the nanoscale level. The area labeled “a” shows fringes at 3.0 Å corresponding to cubic CZ(111) planes related to surface segregated $Ce_{0.70}Zr_{0.30}O_2$. The figure shows also a representative lattice fringe image of the sample along with the Fourier Transform (FT) image corresponding to the area labeled “b”. The FT pattern of this area is complex. The spot at 2.84 Å corresponds well to the (111) spacing of monoclinic $Ce_{0.12}Zr_{0.88}O_2$ phase. Spots at 2.61 Å could be ascribed to (020) planes of monoclinic ZrO_2. However, the spots at 5.22 Å, which are perfectly aligned with the (020) spots and exactly

double the spacing at 2.61 Å, indicate that a supercell exists. Another example of this patterns is shown in the supporting information, Figure S2. To the best of our knowledge no examples of superstructure can be found for monoclinic ZrO_2, while the formation of zirconia oxynitride superstructures was observed when zirconia powders were treated in N_2 at high temperature.[21] There is a very good correspondence between the (200) and (400) lattice fringes measured in the FT images at 5.1-5.2 and 2.5-2.6 Å, respectively, with those reported at 5.066 and 2.533 Å for Zr_2ON_2.[22] The slight differences could be due either to experimental errors and/or to the presence of Ce in the structure. Therefore, the FT can be attributed to a bixbyte-like Zr_2ON_2 structure originated from the insertion of nitrogen into the lattice of zirconia rich phases, with likely inclusion of Ce atoms in the lattice.

XPS analysis (Figure S5) supported the previous findings by revealing a weak, but significative N1s peak at BE energy of *ca*. 399 eV attributable to N in zyrconyl oxynitride phases[23-25]. Further confirmation of the existence of this phase was obtained by analysing the O1s peak (Figure S6). The deconvolution of the O1s band showed a main component at 529.8 eV and a small shoulder at 531.5 eV which have been attributed to oxygen in the solid solution environment and in the zyrconil-oxynitride, respectively.[23]

HRTEM analysis of the sample after the second cycle showed that the zyrconil-oxynitride phase was stable and not disrupted by the water vapor oxidizing atmosphere. The micrograph in Figure 3B clearly shows the presence of the oxynitride phase with the supercell spacings at 3.7 Å and 1.8 Å corresponding to the (220) and (440) crystallographic planes of the structure, respectively. Most of the oxynitride particles measure about 30-50 nm and are very crystalline.

In order to better disclose the role of the oxynitride phase in the production of H_2, we studied for comparison the behavior of a sample calcined in air for 4h at 1300°C. Structural XRD data and surface XPS analysis reveal a situation nearly identical to that observed for the sample treated under nitrogen, Figure 1c and Table 1. Figure 4 shows a representative HRTEM image of this sample with lattice fringes at 3.0 and 1.5 Å corresponding to (111) and (222) crystallographic planes of the cubic $Ce_{0.7}Zr_{0.3}O_2$ phase. At the nanoscale level the catalyst was constituted only by ceria-zirconia crystallites of different structures, and no traces of the presence of oxynitride phase were detected.

In comparison to the catalyst aged under nitrogen, the air treated catalyst showed a lower initial H_2 yield (9 *vs.* 18 µmol/g) and a limited promotional effect (28 *vs.* 109 µmol/g), Figure S7. It turned out that the existence at the nanoscale of the oxynitride phase might have a promotional positive effect on the water splitting reaction mechanism. This promotional effect

can be originated from a good electronic-ionic mixed conductivity of Zr_2ON_2 phase under our operating conditions, which is known to positively affect the water splitting reaction.[26] The insertion of nitrogen in zirconia-rich structures to form a ceria-doped Zr_2ON_2-like phase brings in fact to the formation of vacancies, which, depending on temperature and amount of nitrogen can be randomly oriented or ordered.[27] In addition, N insertion into the ZrO_2 lattice modifies the electronic structure of the oxide.[28] The oxynitride phase can also constitute an intrinsic source of highly active sites for the adsorbtion and activation of water, thanks to the presence of cerium as dopant. Moreover, since nature of the segregated phases and surface characteristics of the material significantly influence the H_2 yield,[29] a synergy between the ceria-rich phase and the oxynitride structure in promoting the adsorption and splitting of water is conceivable. We can hypothesize that the formation of compositional/structural heterogeneities at the nanoscale, favor a reorganization of the surface and the nucleation of more active ceria-zirconia redox centers during the cycles,[30,31] and that these processes are boosted in presence of the oxynitride phase.

The stability of the material was also investigated over six cycles and only a slight decrease of activity was evidenced starting from the last cycle. XPS analysis of the sample after this cycle (Figure S6) evidenced that the zirconium oxynitride phase is still present, but an increase of the Zr/Ce ratio to a value of 2.1 was observed, Table 1. The corresponding X-ray powder difractogram showed a slight redistribution among monoclinic, tetragonal and cubic phases (Table 1 and Figure 1d) and conversely, HRTEM did not reveal the presence of any segregated phase (Figure S3). The results prove that in our specific conditions of testing agglomeration and phases reorganization processes occurred, causing a decrease in cerium content on the surface, that might explain the little deactivation observed.

In summary, a ceria-zirconia oxide with a high amount of Zr (85mol%) was tested in order to evaluate its potential use in the two-step water splitting cycle for H_2 production. The typical temperature adopted in the endothermic step of the cycle induced structural changes with an enrichment in ceria of the surface and an unprecedented formation of a Zr_2ON_2 like phase. These transformations resulted beneficial in both the reduction and oxidation steps. Moreover, redox cycles were found to promote H_2 production. All these findings favourably correlate surface and structural heterogeneity of ceria-zirconia to the increase in hydrogen production after cycling. It is suggested that redox cycling and presence of compositional heterogeneity at a nanoscale level is a key driver in the selection of good candidates for a thermochemical water splitting reaction.

Acknowledgements

L.A. gratefully acknowledges MIUR for financial support through FIRB *Riname* RBAP114AMK project. The Authors thank Dr. Aneggi Eleonora (University of Udine) for Rietveld refinement. J.L. is Serra Húnter Fellow and is grateful to ICREA Academia program and MINECO (ENE2012-36368).

References

[1] Wang, Z.; Roberts R.R.; Naterer G.F.; Gabriel K.S.; Comparison of Thermochemical, Electrolytic, Photoelectrolytic and Photochemical Solar-to-Hydrogen Production Technologies. *Int. J. Hydrogen Energy* **2012**, 37 (21), 16287-16301.

[2] Kodama T.; Gokon N.; Thermochemical Cycles for High-Temperature Solar Hydrogen Production. *Chemical Reviews* **2007**, 107 (10), 4048-4077.

[3] Scheffe J. R.; Steinfeld A.; Oxygen exchange materials for solar thermochemical splitting of H_2O and CO_2: a review. *Mater. Today* **2014**, 17 (7), 341-348.

[4] William C. C.; Sossina M.; Haile, A.; Thermochemical study of ceria: exploiting and old material for new modes of energy conversion and and CO_2 mitigation. *Phil. Trans. R. Soc.* A **2010**, 368, 3269-3294.

[5] Abanades S.; Flamant G.; Thermochemical Hydrogen Production from a Two-Step Solar-Driven Water-Splitting Cycle Based on Cerium Oxides. *Sol. Energy* **2006**, 80 (12), 1611-1623.

[6] Rudisill S. G.; Venstrom L. J.; Petkovich N. D.; Quan T.; Hein N.; Boman D. B.; Davidson J. H.; Stein A.; Enhanced Oxidation Kinetics in Thermochemical Cycling of CeO_2 through templated Porosity. *J. Phys. Chem C* **2013**, 117 (4), 1692-1700.

[7] Kim T.; Vohs J. M.; Gorte R. J. Thermodynamic Investigation of the Redox Properties of Ceria-Zirconia Solid solutions. *Ind. Eng. Chem. Res.* **2006**, 45, 5561-5565.

[8] Zhou G.; Shah P. R.; Kim T.; Fornasiero P.; Gorte J. R. Oxidation entropies and enthalpies of ceria–zirconia solid solutions. *Catal. Today* **2007**, 123, 86-93.

[9] di Monte R.; Kaspar J. Heterogeneous environmental catalysis- a gentle art: CeO_2-ZrO_2 mixed oxide as a case history. *Catal. Today* **2005**, 100, 27-35.

[10] Le Gal A.; Abanades S. Catalytic investigation of ceria-zirconia solid solutions for solar hydrogen production. *Int. J. Hydrogen Energy* **2011**, 36, 4739-4748.

[11] Petkovich N. D.; Rudisill S. G.; Venstrom L.; J.; Boman D. B.; Davidson J. H.; Stein A. Control of Heterogeneity in Nanostructured $Ce_{1-x}Zr_xO_2$ binary oxides for enhanced thermal Stability and water Splitting Activity. *J. Phys. Chem. C* **2011**, 115, 21022-21033.

[12] Kaneko H.; Taku S.; Tamaura T.; Reduction reactivity of CeO_2–ZrO_2 oxide under high O_2 partial pressure in two-step water splitting process. *Solar Energy* **2011**, 85, 2321-2330.

[13] Hao Y.; Yang C-K.; Sossina M. H.; Ceria–Zirconia Solid Solutions ($Ce_{1-x}Zr_xO_{2-\delta}$, $x \leq 0.2$) for Solar Thermochemical Water Splitting: A Thermodynamic Study, *Chem. Mat*. **2014,** 26, 6073-6082.

[14] Jang J.T.; Yoon K.J.; Bae J.W.; Han G. Y.; Cyclic production of syngas and hydrogen through methane-reforming and water-splitting by using ceria–zirconia solid solutions in a solar volumetric receiver–reactor Solar Energy, 2014 109 70–81

[15] Le Gal A.; Abanades S.; Dopants Incorporation in ceria for enhanced water splitting Activity during solar thermochemical Hydrogen generation. *J. Phys. Chem. C* **2012**, 116, 13516-13523.

[16] Le Gal A.; Abanades S.; Bion N.; Le Mercier T.; Harlé V.; Reactivity of doped Ceria-Based Mixed Oxides for solar Thermochemical Hydrogen generation via Two Step Water Splitting Cycles. *Ener. Fuel* **2013**, 27, 6068-6078.

[17] Le Gal A.; Abanades S.; Flamant G.; CO_2 and H_2O splitting for thermochemical production of solar fuels using nonstoichiometric ceria and ceria/zirconia solid solutions. *Energ. fuels* **2011**, 25, 4836-4845.

[18] Yashima M.; Arashi H.; Kakihana M.; Yoshimura M.; Raman Scattering Study of Cubic–Tetragonal Phase Transition in $Zr_{1-x}Ce_xO_2$ Solid Solution. J. Am. Ceram. Soc. 1994, 77 (4), 1067-1071.

[19] Pappacena A.; Schermanz K.; Sagar A.; Aneggi E.; Trovarelli A.; Development of a Modified Co-Precipitation Route for Thermally Resistant, High Surface Area Ceria-Zirconia Based Solid Solutions. *Stud. Surf. Sci. Catal.* **2010,** 175, 835-838.

[20] De Rivas B.; Sampedro C.; Garcia-Real M.; Lopez-Fonseca R.; Gutierrez-Ortiz J.I.;

Promoted activity of sulphated Ce/Zr mixed oxides for chlorinated VOC oxidative abatement

Appl. Catal. B: Env. **2013**, 129, 225– 235

[21] Lerch M., Nitridation of ZrO_2, *J. Am. Ceram. Soc.* **1996**, 79, 2641-2644

[22] Füglein E.; Hock R.; Lerch M., Crystal structure and high temperature behavior of Zr_2ON_2, Z. Anorg. Allg. Chem. **1997**, 623, 304-308.

[23] Cubillos G.I., Bethencourt M.; Olaya J.J.; Corrosion resistance of zirconium oxynitride coatings deposited via DC unbalanced magnetron sputtering and spray pyrolysis-nitriding *Appl. Surf. Sci.* **2015,** 327 288–295

[24] Rizzo A.; Signore M.A.; Mirenghi L.; Tapfer L.; Piscopiello E.; Salernitano E.; Giorgi R.; Sputtering deposition and characterization of zirconium nitride and oxynitride films *Thin Solid Films* **2012**, 520, 3532–3538

[25] Rizzo A.; Signore M.A.; Mirenghi L.; Piscopiello E.; Tapfer L.; Physical properties evolution of sputtered zirconium oxynitride films: effects of the growth temperature *J. Phys. D: Appl. Phys.* **2009,** 42 art *235401*(pp8).

[26] Meng Q.-L.; Lee C.-il; Ishihara T.; Kaneko H.; Tamaura Y.; Reactivity of CeO_2-based ceramics for solar hydrogen production via a two-step water-splitting cycle with concentrated solar energy; *Int.J. Hydrogen Energy*, **2011**, 36, 13435-13441

[27] Clarke S. J.; Michie C. W.; Rosseinsky M. J.; Structure of $Z_{r2}ON_2$ by Neutron Powder Diffraction: The Absence of Nitride/Oxide Ordering. *J. Solid State Chem.*, **1999**,146, 399-405

[28] Mishima T.; Matsuda M.; Miyake M.; Visible-light photocatalytic properties and electronic structure of Zr-based oxynitride, Zr_2ON_2, derived from nitridation of ZrO_2, *Appl. Catal. A: Gen.*, **2007**, 324, 77–82

[29] Pappacena A.; Boaro M.; Šolcová O.; Trovarelli A.; Ceria Based Materials with Enhanced OSC Properties for H_2 Production by Water Splitting Reaction proceeding. *Adv. Sci. Tech*. **2014**, 93, 76-81.

[30] Yeste M.P.; Hernandez-Garrido J.C.; Arias D.C.; Blanco G.; Rodriguez-Izquierdo J.M.; Pintado J. M.; Bernal S.; Perez Omil J.A.; Calvino J.J.; Rational design of nanostructured , noble metal free, ceria-zirconia catalysts with outstanding low temperature oxygen storage capacity. *J. Mater. Chem. A* **2013**, 1, 4836-4844.

[31] Wang R.; Crozier P.A.; Sharma R.; Nanoscale compositional and structural evolution in ceria zirconia durinf cycling redox treatments, *J. Mater Chem*. **2010,** 20, 7497-7505.

Captions of figures and Tables

Figure 1: X-ray difractograms of catalyst: a) calcined at 500°C, b) treated at 1300°C in N_2 flow for 4 h, c) treated at 1300°C in air flow for 4h d) treated at 1300°C in N_2 flow for 4 h and tested over six redox cycles; ▼ monoclinic phase, ■ cubic phase, ◆ tetragonal phase.

Figure 2: H_2 production over six redox cycles at 800°C of the sample treated in N_2 at 1300°C for 4 hours.

Figure 3: A. HRTEM images of the sample treated in N_2 flow at 1300°C for 4 hours, before testing; B. HRTEM image of sample treated in N_2 flow at 1300°C for 4 hours and tested in water splitting conditions (reduction in 5%H_2 in Ar at 800°C, Oxidation at 800°C with 30% water vapor in He) for two cycles.

Figure 4: HRTEM image of sample treated in air flow at 1300°C for 4 hours

Figure 1:

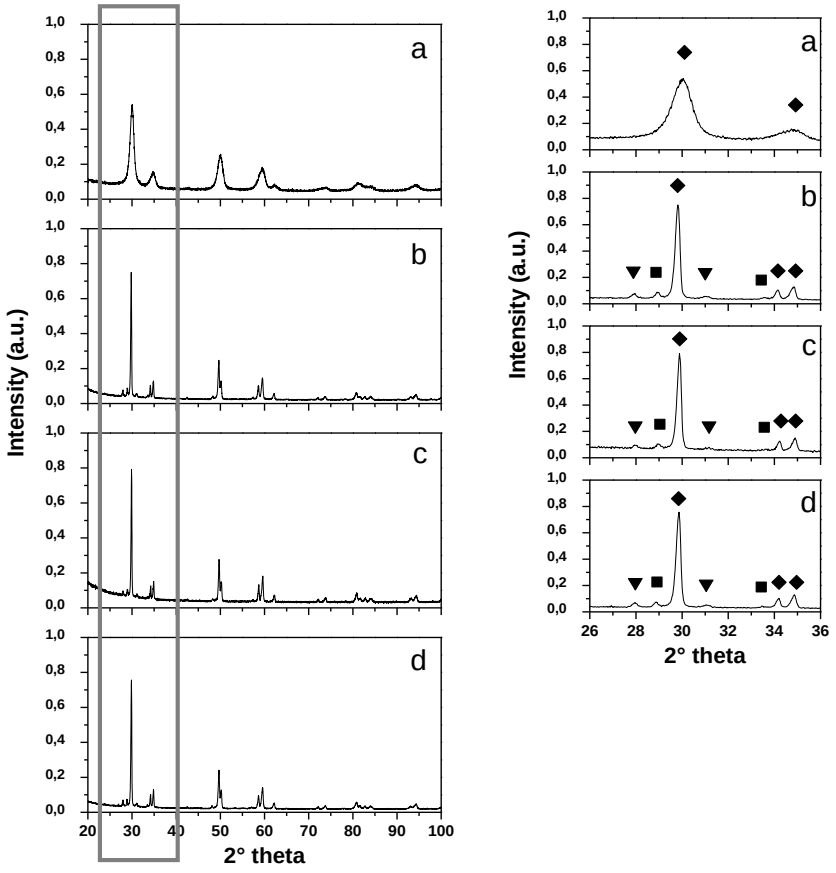

Figure 2

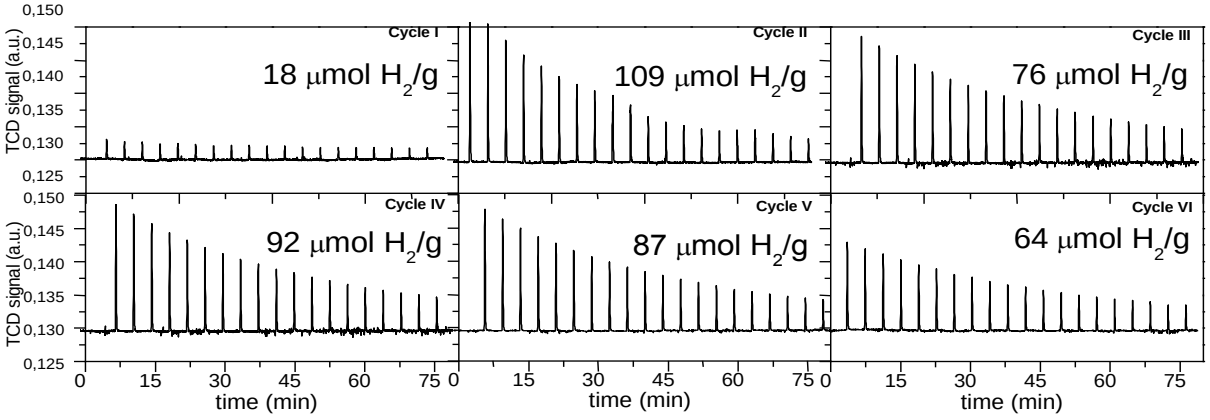

Figure 3

A)

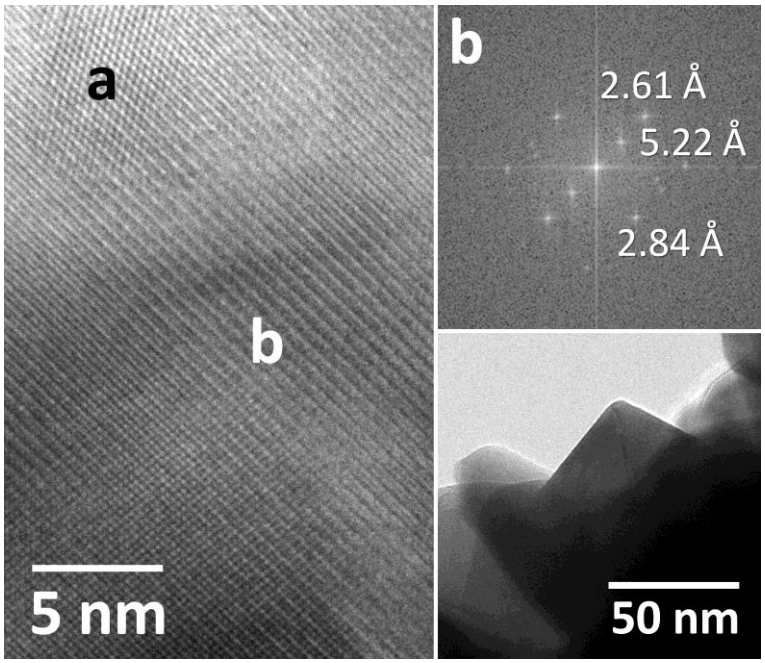

B)

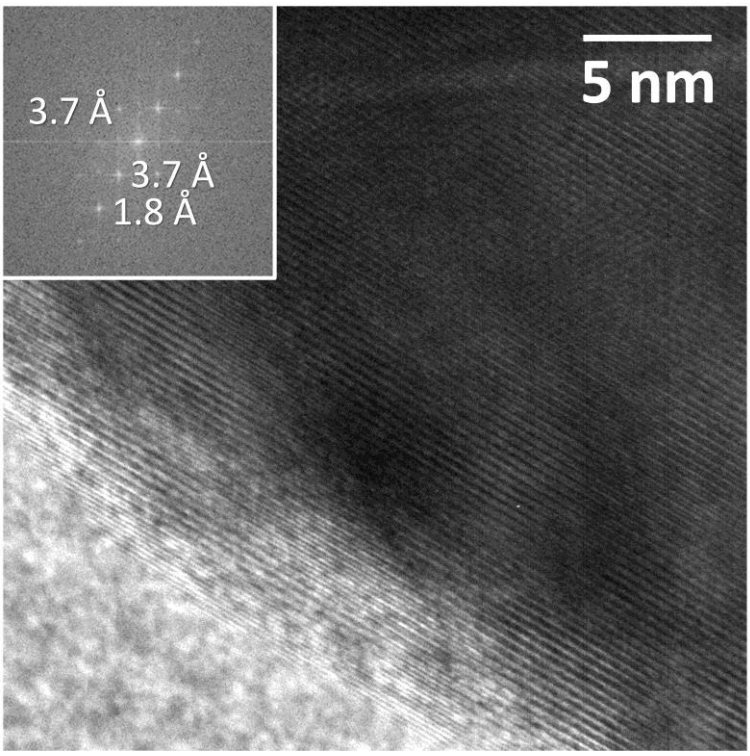

Figure 4

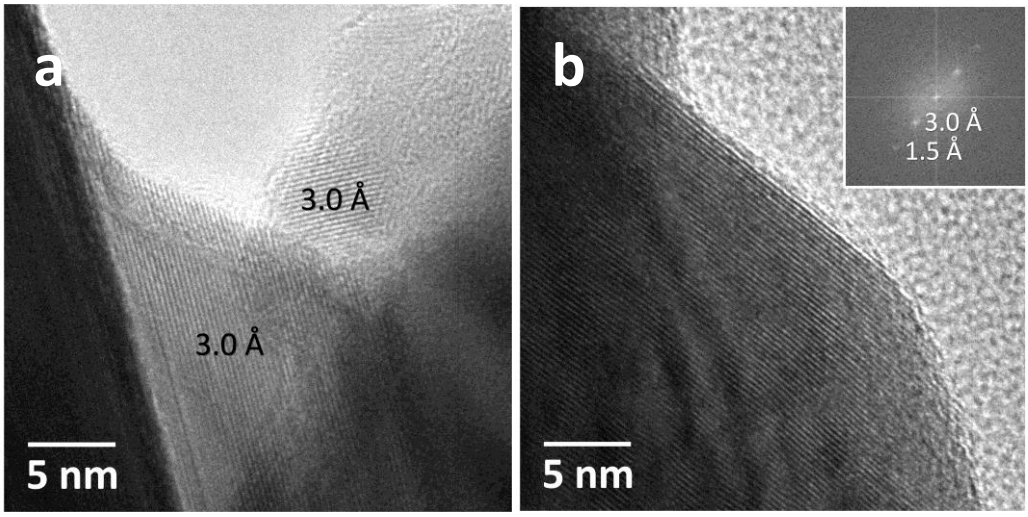

Table 1. Structural and surface characterization obtained from XRD and XPS measurements.

samples	XRD phase composition			XPS Zr/Ce
	Tetragonal $Ce_{0.15}Zr_{0.85}O_2$	Monoclinic $Ce_{0.12}Zr_{0.88}O_2$	Cubic $Ce_{0.70}Zr_{0.30}O_2$	*atom%*
N_2-aged	89.8 ± 0.10	8.6 ± 0.4	1.6 ± 0.1	~ 1.8
Air-aged	88.3 ± 0.10	8.9 ± 0.5	2.8 ± 0.2	~ 1.8
Cycled	93.1 ± 0.10	4.8 ± 0.6	2.1 ± 0.2	~ 2.1